LU-TP 14-37
November 2014

Status of Chiral Meson Physics[†]

Johan Bijnens

Department of Astronomy and Theoretical Physics, Lund University,
Sölvegatan 14A, SE 223-62 Lund, Sweden

Abstract

This talk includes a short introduction to Chiral Perturbation Theory in the meson sector concentrating on a number of recent developments. I discuss the latest fit of the low-energy constants. Finite volume corrections are discussed for the case with twisted boundary conditions for form-factors and first results at two-loops for three flavours for masses. The last part discusses the extension to other symmetry breaking patterns relevant for technicolour and related theories as well as the calculation of leading logarithms to high loop orders.

[†] Plenary talk at "XIth Quark Confinement and the Hadron Spectrum, Saint-Petersburg, Russia, 8-12 September 2014.

Status of Chiral Meson Physics

Johan Bijnens

Department of Astronomy and Theoretical Physics, Lund University, Sölvegatan 14A, SE 22362 Lund, Sweden

Abstract. This talk includes a short introduction to Chiral Perturbation Theory in the meson sector concentrating on a number of recent developments. I discuss the latest fit of the low-energy constants. Finite volume corrections are discussed for the case with twisted boundary conditions for form-factors and first results at two-loops for three flavours for masses. The last part discusses the extension to other symmetry breaking patterns relevant for technicolour and related theories as well as the calculation of leading logarithms to high loop orders.

Keywords: Chiral perturbation Theory, Effective Lagrangians
PACS: 11.30.Rd,12.39.Fe,12.60.Nz,13.40.Gp,14.40.Be,14.40.Df

1. INTRODUCTION

This talk is an overview of mesonic Chiral Perturbation Theory (ChPT) concentrating on a number of recent developments.

2. CHIRAL PERTURBATION THEORY

Chiral Perturbation Theory can best be described by "Exploring the consequences of the chiral symmetry of QCD and its spontaneous breaking using effective field theory techniques." It was introduced by Weinberg, Gasser and Leutwyler [1, 2, 3]. A good discussion of the underlying assumptions can be found in [4]. References to lectures and other material can be found in [5].

A general effective field theory (EFT) needs three principles: the correct degrees of freedom, there has to be a power-counting principle to ensure predictivity and one should remember the associated range of validity. For ChPT the degrees of freedom are the Nambu-Goldstone bosons from the spontaneous symmetry breaking of the chiral symmetry of massless QCD, the power-counting for mesonic ChPT is dimensional counting in momenta and meson masses, and the range of validity stops somewhere below the mass of the first not included resonance, the rho.

The QCD Lagrangian

$$\mathscr{L}_{QCD} = \sum_{q=u,d,s} [i\bar{q}_L \not{D} q_L + i\bar{q}_R \not{D} q_R - m_q(\bar{q}_R q_L + \bar{q}_L q_R)] \tag{1}$$

has an $SU(3)_L \times SU(3)_R$ global chiral symmetry when $m_q = 0$. This symmetry is spontaneously broken by the quark-antiquark vacuum-expectation-value $\langle \overline{q}q \rangle = \langle \overline{q}_L q_R \overline{q}_R q_L \rangle \neq 0$. The mechanism is discussed in the talk by L. Giusti. The remaining symmetry group is $SU(3)_V$, we have thus 8 broken generators and get 8 Goldstone bosons whose interaction vanishes at zero momentum. The latter allows for a consistent power counting via dimensional counting [1].

There are many extensions of ChPT in different directions. Some of them are:

- Which chiral symmetry: $SU(N_f)_L \times SU(N_f)_R$, for $N_f = 2, 3, \ldots$ and extensions to (partially) quenched
- Or beyond QCD
- Space-time symmetry: Continuum or broken on the lattice: Wilson, staggered, mixed action
- Volume: Infinite, finite in space, finite T
- Which interactions to include beyond the strong one
- Which particles included as non Goldstone Bosons

My general belief is that if it involves soft pions (or soft K, η) some version of ChPT exists.

TABLE 1. The number of low-energy constants (LECs) at each order in the expansion for a number of cases, the $i+j$ notation indicates the number of mesonic + pure contact terms.

order	2 flavour		3 flavour		PQChPT/N_f flavour	
p^2	F,B	2	F_0,B_0	2	F_0,B_0	2
p^4	l_i^r,h_i^r	7+3	L_i^r,H_i^r	10+2	$\hat{L}_i^r,\hat{H}_i^r$	11+2
p^6	c_i^r	52+4	C_i^r	90+4	K_i^r	112+3

The Lagrangians are written in terms of the special unitary matrix, parametrizing $SU(3)_\times SU(3)_R/SU(3)_V \approx SU(3)$,

$$U = e^{i\sqrt{2}\Phi/F_0} \quad \text{with} \quad \Phi(x) = \begin{pmatrix} \frac{\pi^0}{\sqrt{2}} + \frac{\eta_8}{\sqrt{6}} & \pi^+ & K^+ \\ \pi^- & -\frac{\pi^0}{\sqrt{2}} + \frac{\eta_8}{\sqrt{6}} & K^0 \\ K^- & \bar{K}^0 & -\frac{2\,\eta_8}{\sqrt{6}} \end{pmatrix}. \tag{2}$$

In terms of these the lowest order Lagrangian is given by

$$\mathscr{L}_2 = \frac{F_0^2}{4}\{\langle D_\mu U^\dagger D^\mu U\rangle + \langle \chi^\dagger U + \chi U^\dagger\rangle\}, \tag{3}$$

with $D_\mu U = \partial_\mu U - i r_\mu U + i U l_\mu$, and $\chi = 2B_0(s+ip)$ in terms of the left and right external currents: $r(l)_\mu = v_\mu + (-)a_\mu$ and scalar and pseudo-scalar external densities: s,p [3]. Quark masses are included via the scalar density: $s = \mathscr{M} + \cdots$. The notation $\langle A\rangle = Tr_F(A)$ indicates the trace over flavours.

At higher orders many more terms appear. The number of terms is listed in Tab. 1. The free coefficients of those terms are called low-energy constants (LECs). The two- and three-flavour p^4 Lagrangians were constructed in [2, 3], the p^6 Lagrangians in [6]. Including finite volume and boundary conditions does not introduce any new LECs, other effects and interactions typically introduce (many) new LECs.

Let me just add a reminder about the main properties of ChPT: It relates processes with different numbers of pseudo-scalars, includes isospin and the eightfold way ($SU(3)_V$) and unitarity and analyticity effects are included perturbatively. The best known consequence are the chiral logarithms, e.g. for the example of the pion mass [2]

$$m_\pi^2 = 2B\hat{m} + \left(\frac{2B\hat{m}}{F}\right)^2 \left[\frac{1}{32\pi^2}\boxed{\log\frac{(2B\hat{m})}{\mu^2}} + 2l_3^r(\mu)\right] + \cdots \tag{4}$$

with $M^2 = 2B\hat{m}$ the lowest-order mass.

3. DETERMINATION OF LECS IN THE CONTINUUM

One of the problems in practically using ChPT is to have values for the unknown LECs. The original determination was done in [2, 3] at the p^4 level. However, all needed observables are known to order p^6, as reviewed in [7]. The latest update of the LECs can be found in [8].

The two-flavour constants, quoted in the subtraction-scale-independent form $\bar{l}_i$, are

$$\begin{aligned} \bar{l}_1 &= -0.4 \pm 0.6, & \bar{l}_2 &= 4.3 \pm 0.1, & \bar{l}_3 &= 3.0 \pm 0.8, & \bar{l}_4 &= 4.3 \pm 0.2, \\ \bar{l}_5 &= 12.24 \pm 0.21, & \bar{l}_6 - \bar{l}_5 &= 3.0 \pm 0.3, & \bar{l}_6 &= 16.0 \pm 0.5 \pm 0.7. \end{aligned} \tag{5}$$

$\bar{l}_1$ and $\bar{l}_2$ follow from the $\pi\pi$-scattering analysis [9], see also [10]. $\bar{l}_3$ is mainly restricted from lattice data [11] and $\bar{l}_4$ from the quark mass dependence of F_π and the pion scalar radius [12]. $\bar{l}_5 - \bar{l}_6$ is from the pion electromagnetic radius [12], while $\bar{l}_5$ follows from the decay $\pi \to e\nu\gamma$[13] and τ-decays [14].

The three flavour first full p^6 fit was done in [15, 16]. Including many more observables and new data, a major update was done by [17] and a final update with the same experimental input but some more information on p^6 LECs

TABLE 2. Values of the p^4 three-flavour ChPT LECs, L_i^r in the major fits performed at two-loop order. dof stands for degrees of freedom.

	ABC01	JJ12	L_4^r free	BE14
	old data			
$10^3 L_1^r$	0.39(12)	0.88(09)	0.64(06)	0.53(06)
$10^3 L_2^r$	0.73(12)	0.61(20)	0.59(04)	0.81(04)
$10^3 L_3^r$	−2.34(37)	−3.04(43)	−2.80(20)	−3.07(20)
$10^3 L_4^r$	$\equiv 0$	0.75(75)	0.76(18)	$\equiv 0.3$
$10^3 L_5^r$	0.97(11)	0.58(13)	0.50(07)	1.01(06)
$10^3 L_6^r$	$\equiv 0$	0.29(8)	0.49(25)	0.14(05)
$10^3 L_7^r$	−0.30(15	−0.11(15)	−0.19(08)	−0.34(09)
$10^3 L_8^r$	0.60(20)	0.18(18)	0.17(11)	0.47(10)
χ^2	0.26	1.28	0.48	1.04
dof	1	4	?	?
F_0 [MeV]	87	65	64	71

in [8]. Recent values of the weak interaction ChPT LECs can be found in [18, 19]. An overview of the lattice work is the FLAG second report [11].

For the three-flavour case we have that $m_K^2, m_\eta^2 >> m_\pi^2$ so a question is whether ChPT works at all in this sector. The contributions from the not very well known p^6 LECs are much larger and there is the question of the importance of $1/N_c$ suppressed terms. In [20] a large number of observables was checked and a number of relations found that were independent of the p^6 LECs and only depend on p^4 LECs via loop contributions. With 76 observables we found 35 relations. For 13 of these there were enough experimental data available. The resulting picture was that three-flavour ChPT works but might converge slowly in some cases.

The data included for a fit of $L_1^r, \cdots, L_8^r$ are:

- $M_\pi, M_K, M_\eta, F_\pi, F_K/F_\pi$
- $\langle r^2 \rangle_S^\pi$, c_S^π slope and curvature of F_S
- $\pi\pi$ and πK scattering lengths a_0^0, a_0^2, $a_0^{1/2}$ and $a_0^{3/2}$.
- Value and slope of F and G in $K_{\ell 4}$
- $\frac{m_s}{\hat{m}} = 27.5$ (lattice)
- $\bar{l}_1, \ldots, \bar{l}_4$

This corresponds to $17+3$ inputs and we have 8 L_i^r and 34 combinations of C_i^r to fit, a clearly ill-defined problem. The older fits [16] (ABC01), [17](BJ12) used a simple resonance estimate of the C_i^r, this was complemented by more input on the C_i^r from other models and various estimates and a requirement of not too large p^6 corrections the meson masses in [8] (BE14). The resulting values of the fits are shown in Tab. 2.

Many prejudices, as described in detail in [8], were used in fixing the values of the C_i^r. The final values chosen are all "reasonable" and compatible with existing determinations. The large N_c suppressed constant L_4^r, if left free, is rather large. We therefore restricted it to the expected range. Surprisingly, this lead to the values of L_6^r and $2L_1^r - L_2^r$ also being small and compatible with large N_c arguments. The values for the L_i^r are compatible with existing lattice determinations as well. The convergence is reasonable, but enforced for the masses, as can be seen from the examples:

$$
\begin{aligned}
\text{Mass:} \qquad m_\pi^2/m_{\pi phys}^2 &= 1.055(p^2) - 0.005(p^4) - 0.050(p^6)\,, \\
m_K^2/m_{K phys}^2 &= 1.112(p^2) - 0.069(p^4) - 0.043(p^6)\,, \\
m_\eta^2/m_{\eta phys}^2 &= 1.197(p^2) - 0.214(p^4) + 0.017(p^6)\,, \\
\text{Decay constants:} \qquad F_\pi/F_0 &= 1.000(p^2) + 0.208(p^4) + 0.088(p^6)\,, \\
F_K/F_\pi &= 1.000(p^2) + 0.176(p^4) + 0.023(p^6)\,. \\
\text{Scattering:} \qquad a_0^0 &= 0.160(p^2) + 0.044(p^4) + 0.012(p^6)\,, \\
a_0^{1/2} &= 0.142(p^2) + 0.031(p^4) + 0.051(p^6)\,. \qquad (6)
\end{aligned}
$$

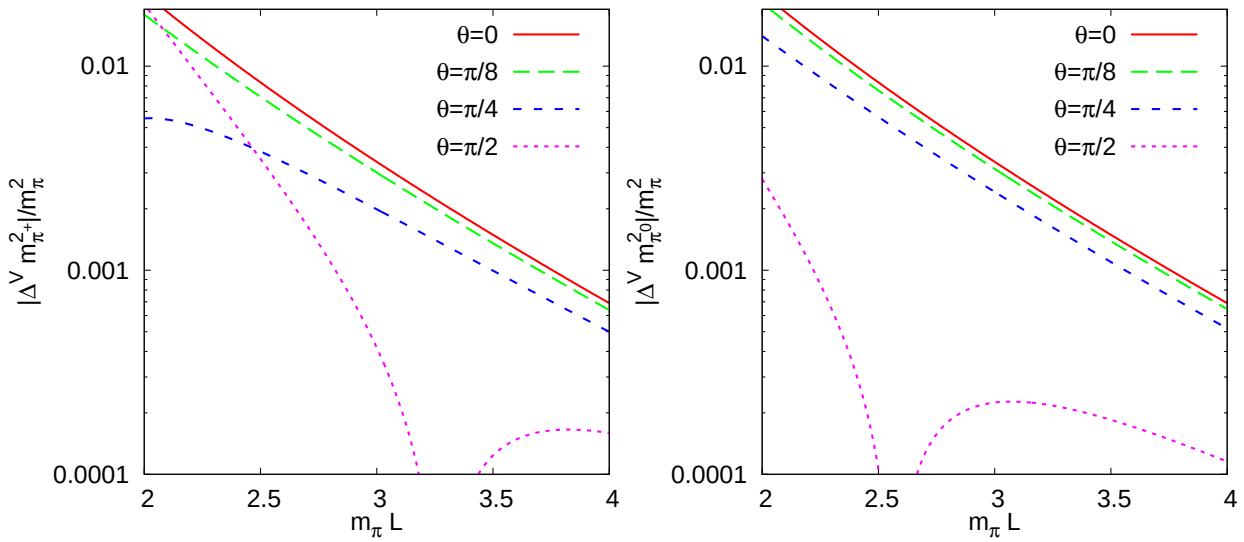

FIGURE 1. Finite volume corrections to the charged and neutral pion mass squared as a function of $m_\pi L$ for several values of the up quark twist angle θ. (a) Charged pion (b) neutral pion. Plots from [33].

4. FINITE VOLUME

An example of extra effects that can be included is the use of ChPT to study the effects of a finite volume. Finite volume effects were studied first in a general way by Lüscher [21] and soon introduced in ChPT by Gasser and Leutwyler [22, 23]. In particular, [23] proved that no new LECs were needed. They calculated m_π, F_π and $\langle\bar{q}q\rangle$ to one-loop in the equal mass case. Note that the remainder will be in the p-regime with $m_\pi L \geq 1$. L is the size of the finite volume. ChPT will be useful since the convergence is given by the rho mass with $1/m_\rho \approx 0.25$ fm, while the finite volume effects are controlled by $1/m_\pi \approx 1.4$ fm. It will often be needed to go beyond the leading $\exp(-m_\pi L)$ behaviour. An introduction and more references can be found in [24].

A partial overview of existing results at finite volume is: Masses and decay constants for three flavours at one-loop [25, 26, 27], m_π at two-loop order in two-flavour ChPT [28] and the quark-anti-quark vacuum-expectation value at two-loops in three-flavour ChPT [29]. Other examples are including a twisted mass [30] and twisted boundary conditions [31] in ChPT. I will now concentrate on two recent developments.

4.1. Twisted boundary conditions

On a lattice with a finite size given by L, components of spatial momenta are restricted by $p^i = 2\pi n^i/L$ with n^i integer. That means that in practice very few low momenta are available. One way to allow for more momenta is to put a boundary condition on some of the quark fields in some directions via $q(x^i + L) = e^{i\theta^i_q} q(x^i)$. Then allowed momenta are $p^i = \theta^i/L + 2\pi n^i/L$. Varying the θ^i_q allows to map out momentum space on the lattice much better [32]. The finite box breaks rotational symmetry down to cubic symmetry but twisting reduces it even further. Consequences are:

- $m^2(\vec{p}) = E^2 - \vec{p}^2$ is not constant.
- There are typically more form-factors than in infinite volume.
- In general quantities can depend on many more components of the momenta, not just Lorentz-invariant products.
- Charge conjugation involves a change in momentum.
- The boundary conditions can break isospin.

As a first example I show the finite volume corrections to the charged and neutral pion mass [33] in Fig. 1. The plots show the finite volume correction $\Delta^V m^2 = m^{2V} - m^{2V=\infty}$ as a function of $m_\pi L$ for several values of θ with $\vec{\theta}_u = (\theta, 0, 0)$

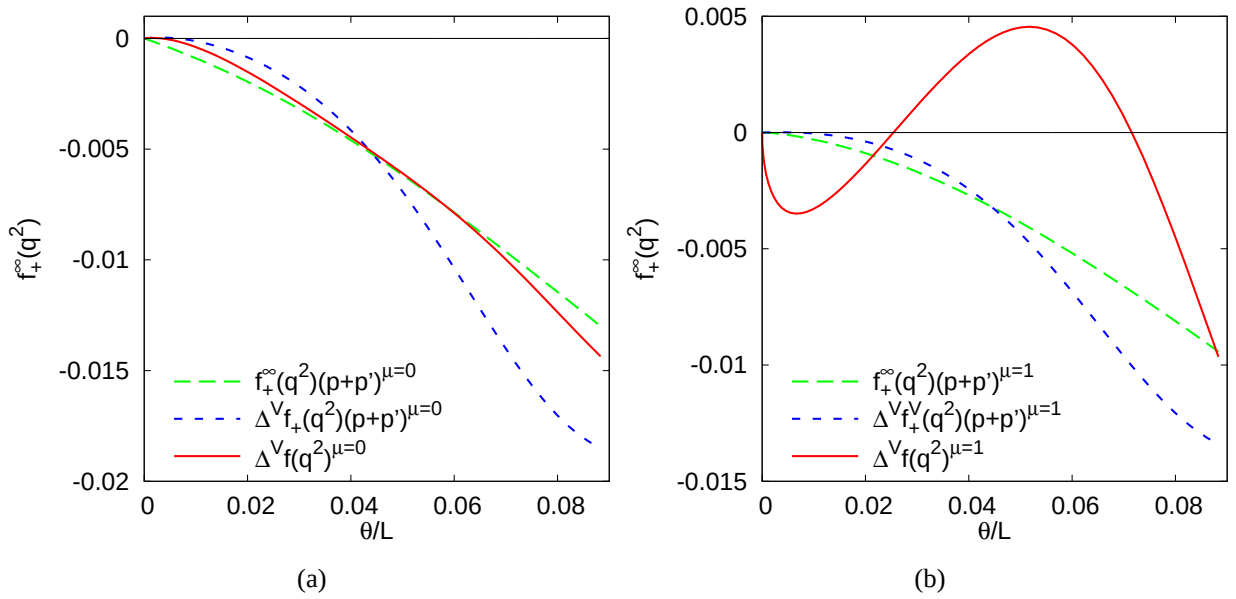

(a) (b)

FIGURE 2. Finite volume corrections and infinite volume one-loop part of the components of the π^+-π^0 vector transition form-factors. (a) $\mu = t$ component (b) $\mu = x$ component. Plots from [33].

and $\vec{\theta}_d = \vec{\theta}_s = 0$. The relation with the earlier work in [31] and [34] is discussed in detail in [33]. Note that the finite volume correction is very dependent on the twist-angle.

The matrix-element for the decay constant has extra terms

$$\langle 0|A_\mu^M|M(p)\rangle = i\sqrt{2}F_M p_\mu + i\sqrt{2}F_{M\mu}^V\,. \tag{7}$$

These are required such that the Ward identities are satisfied [33] and the extra components can be quite sizable.

The vector-form factors also require extra components [33]:

$$\langle M'(p')|j_\mu|M(p)\rangle = f_\mu = f_+(p_\mu + p'_\mu) + f_- q_\mu + h_\mu\,. \tag{8}$$

earlier work on two flavours is [34]. Note that the vector current satisfies the Ward identities, contrary to what is sometimes stated but $q^\mu f_\mu = (p^2 - p'^2) f_+ + q^2 f_- + q^\mu h_\mu = 0$ requires to include all components and the use of the correct finite volume masses for p^2 and p'^2.

The lattice determination of the pion electromagnetic form-factor from the π^+-π^0 transition amplitude

$$f_\mu = -\frac{1}{\sqrt{2}}\langle \pi^0(p')|\bar{d}\gamma_\mu u|\pi^+(p)\rangle = \left(1 + f_+^\infty + \Delta^V f_+\right)(p+p')_\mu + \Delta^V f_- q_\mu + \Delta^V h_\mu \tag{9}$$

requires all the finite volume corrections. In Fig. 2 the corrections needed are shown for the time and x spatial component of the form-factor f_μ of (9). Plotted is also for comparison the pure one-loop contribution to the infinite volume form-factor f_+^∞.

4.2. Masses at two-loops

The finite volume correction for the meson masses and decay constants in three-flavour ChPT is in progress [35]. As was already visible in the two-flour two-loop calculation of [28], the main obstacle for a full two-loop calculation is the finite volume sunset integrals. These were derived for the most general mass case in [36], thus paving the way for a full two-loop evaluation. Some preliminary results are shown in Fig. 3. For the pion mass at order p^4 the two- and three-flavour result differ by kaon and eta loops. These are numerically very small. The p^6 results are also in good agreement with each other. The kaon mass at order p^4 has only a very small correction since there is no pion-loop

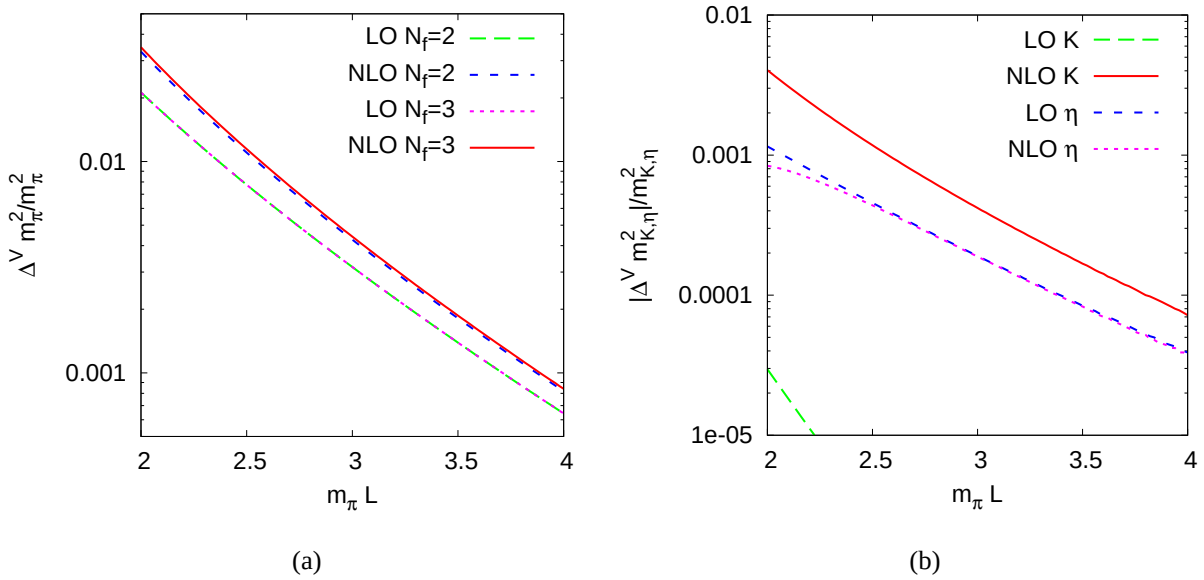

(a) (b)

FIGURE 3. Finite volume corrections at two-loop order to the meson masses squared. Shown is the relative correction $\Delta^V m_\pi^2/m_\pi^2 = m_\pi^{V2}/m_\pi^{V=\infty 2} - 1$. LO is the p^4 or one-loop results. NLO is the p^6 or two-loop result. (a) Pion mass in two- and three-flavour ChPT (b) Kaon and eta mass.

contribution. The p^6 contribution is of the expected size. For the η, there is a cancellation between the pure two-loop contribution and the L_i^r-dependent part at p^6 resulting in a very small correction in total. The p^4 contribution is suppressed by an extra factor of m_π^2/m_η^2. More results and details will be published in [35].

5. BEYOND QCD

There are other symmetry breaking patterns possible in generic gauge theories. Early examples are related to technicolour [37, 38, 39] and some might be useful to avoid the sign problem in high density QCD lattice simulations [40]. The equal mass case requires for many quantities the same integrals as needed for $\pi\pi$-scattering in two-flavour ChPT [41, 42]. The lattice studies of these type of theories was discussed in the talk by E. Pallante. One often wants to extrapolate to zero fermion masses from the lattice data here. ChPT can help there, just as for the QCD case. A number of quantities were studied for N equal mass flavours for the complex, real and pseudo-real case [43, 44, 45] at two-loop order. References to earlier one-loop work can be found in our work and [40].

Generically the fermions can be in a complex, real or pseudo-real representation of the gauge group. Examples are of the first case QCD, the second case any group with fermions in the adjoint representation and the last case an $SU(2)$ gauge group with fermions in the fundamental representation. In the latter two cases anti-quarks are in the same representation as the quarks leading to larger global chiral symmetry group. Assuming that a condensate forms similar to QCD, we get the breaking patterns:

- $SU(N) \times SU(N)/SU(N)$ (complex)
- $SU(2N)/SO(2N)$ (real)
- $SU(2N)/Sp(2N)$ (pseudo-real)

The three cases can be dealt with in very similar fashion.

The standard QCD case has a vector $q^T = (q_1 \cdots q_{N_F})$ and the chiral symmetry transformation under $(g_L, g_R) \in G = SU(N_F)_L \times SU(N_F)_R$ is $q_L \to g_L q_L, q_R \to g_R q_R$. The condensate $\langle \overline{q}_{Lj} q_{Ri} \rangle = -v\Sigma_{ij}$ is described by a unitary matrix Σ. The vacuum expectation value is $\langle \Sigma \rangle = 1$, the unity matrix, such that for $g_L = g_r$ the vacuum remains invariant under $\Sigma \to g_R \Sigma g_L^\dagger$. The conserved symmetry group is thus $H = SU(N_F)_V$.

The case with N_F fermions in a real representation of the gauge group can be described by a $2N_F$ vector $\hat{q}^T = (q_{R1} \ \ldots \ q_{RN_F} \ \tilde{q}_{R1} \ \ldots \ \tilde{q}_{RN_F})$ with $\tilde{q}_{Ri} \equiv C\overline{q}_{Li}^T$. C is charge conjugation. The global chiral symmetry is thus $G = SU(2N_F)$

with $\hat{q} \to g\hat{q}$. The vacuum expectation value $\langle \overline{q}_j q_i \rangle$ is really

$$\Sigma_{ji} = \langle (\hat{q}_j)^T C \hat{q}_i \rangle \propto J_{Sij} \qquad \text{with} \qquad J_S = \begin{pmatrix} 0 & I \\ I & 0 \end{pmatrix}. \tag{10}$$

Σ is $2N_F \times 2N_F$ and $\Sigma \to g\Sigma g^T$ for $g \in G$. The vacuum is conserved if $gJ_S g^T = J_S \Longrightarrow$. The conserved part is $H = SO(2N_F)$.

For N_F fermions in a pseudo-real representation the situation is similar but $\hat{q}^T = (q_{R1} \ \ldots \ q_{RN_F} \ \tilde{q}_{R1} \ \ldots \ \tilde{q}_{RN_F})$ with $\tilde{q}_{R\alpha i} \equiv \varepsilon_{\alpha\beta} C \overline{q}^T_{L\beta i}$ instead. q_{Ri} transforms under the gauge group as $q_{R\alpha i}$. The global chiral symmetry is thus again $G = SU(2N_F)$ with $\hat{q} \to g\hat{q}$. The vacuum expectation value $\langle \overline{q}_j q_i \rangle$ corresponds now to

$$-v\Sigma_{ji} = \varepsilon_{\alpha\beta} \langle (\hat{q}_{\alpha j})^T C \hat{q}_{\beta i} \rangle \propto J_{Aij} \qquad \text{with} \qquad J_A = \begin{pmatrix} 0 & -I \\ I & 0 \end{pmatrix}. \tag{11}$$

Σ is again a $2N_F \times 2N_F$ matrix and $\Sigma \to g\Sigma g^T$ for $g \in G$. The vacuum is conserved if $gJ_A g^T = J_A$ with a conserved global symmetry $H = Sp(2N_F)$.

ChPT for the three cases is extremely similar if we define $u = \exp(i\phi^a X^a / (\sqrt{2}F))$ [43] with the X^a the generators of an $SU(N_F)$ (complex case), or of an $SU(2N_F)$ satisfying $X^a J_S = J_S X^{aT}$ (real) or $X^a J_A = J_A X^{aT}$ (pseudo-real). Note that these are not the usual ways of parametrizing $Sp(2N_F)$ or $SO(2N_F)$ matrices but related. As a consequence the Lagrangians constructed for the N_F flavor complex case [6] can be taken, but might not be minimal. Also the divergence structure for the complex case is known [46], providing a check on the calculations.

The expressions for masses, decay constants and vacuum expectation values to two-loop order can be found in [43] and are known fully analytically. The meson-scattering case can be written in terms of two amplitudes $B(s,t,u)$ and $C(s,t,u)$ [44], analoguous to $A(s,t,u)$ defined in $\pi\pi$-scattering, see e.g. [41]. The possible intermediate states are a little more complicated than for $\pi\pi$-scattering. All scattering formulas are fully analytically obtained in [44]. For explicit expressions I refer to that paper. As an example, I show the single meson-scattering length as a function of $n = N_F$ for the complex case in Fig. 4.

The last application we did was to perform the calculations necessary to extract the S-parameter [45].

6. LEADING LOGARITHMS

The last application is the calculation of leading logarithms (LL) in EFT and especially mesonic ChPT. Leading logarithms are the following, take as an example an observable quantity F dependent on a single physical scale M. The dependence on the subtraction scale μ in field theory is typically logarithmic:

$$F = F_0 + F_1^1 L + F_0^1 + F_2^2 L^2 + F_1^2 L + F_0^2 + F_3^3 L^3 + \cdots \qquad L = \log(\mu/M). \tag{12}$$

The coefficients F_j^i are i loop-level and j logarithm-level. The terms with F_m^m are called the leading logarithm terms. These terms are easier to calculate than the remaining ones at the same loop level. The underlying reason is that physical quantities must be independent of the subtraction scale, $\mu\,(dF/d\mu) \equiv 0$ and that divergences in local quantum field theory are always local.

In a renormalizable quantum field theory the leading logarithms can be calculated by a simple one-loop calculation using the renormalization group. In an EFT this is not quite so simple since at each order in the expansion new terms in the Lagrangian occur. Weinberg [1] showed that the leading logarithms at two-loop level could be obtained from one-loop calculations only. The full two-loop leading logarithm was calculated with these Weinberg consistency conditions in [47]. This was expected to work similarly to all orders and proven to do so in [48], an alternative diagrammatic proof is in [49]. The underlying argument is that at n-loop order, ($\overline{h}^n$), all the divergences must cancel. For $d = 4 - w$ all terms of the form $1/w^i \log^j \mu$ with $i = 1, \ldots, n$ and $j = 0, \ldots, n-1$ must cancel. For the leading logarithms the n conditions with $i + j = n$ give a sufficient amount of relations that the leading logarithms can be obtained from one-loop diagrams only, the conditions with $i + j = n - 1$ show that for the next-to-leading logarithms two-loop diagrams are required and so on.

The problem is that each order new terms in the Lagrangians show up, so new one-loop diagrams are required and new vertices at each new order. The problem is illustrated in Fig. 5 for the case of the mass at two-loop order. We need in general both new vertices of higher order but also new vertices with more external legs.

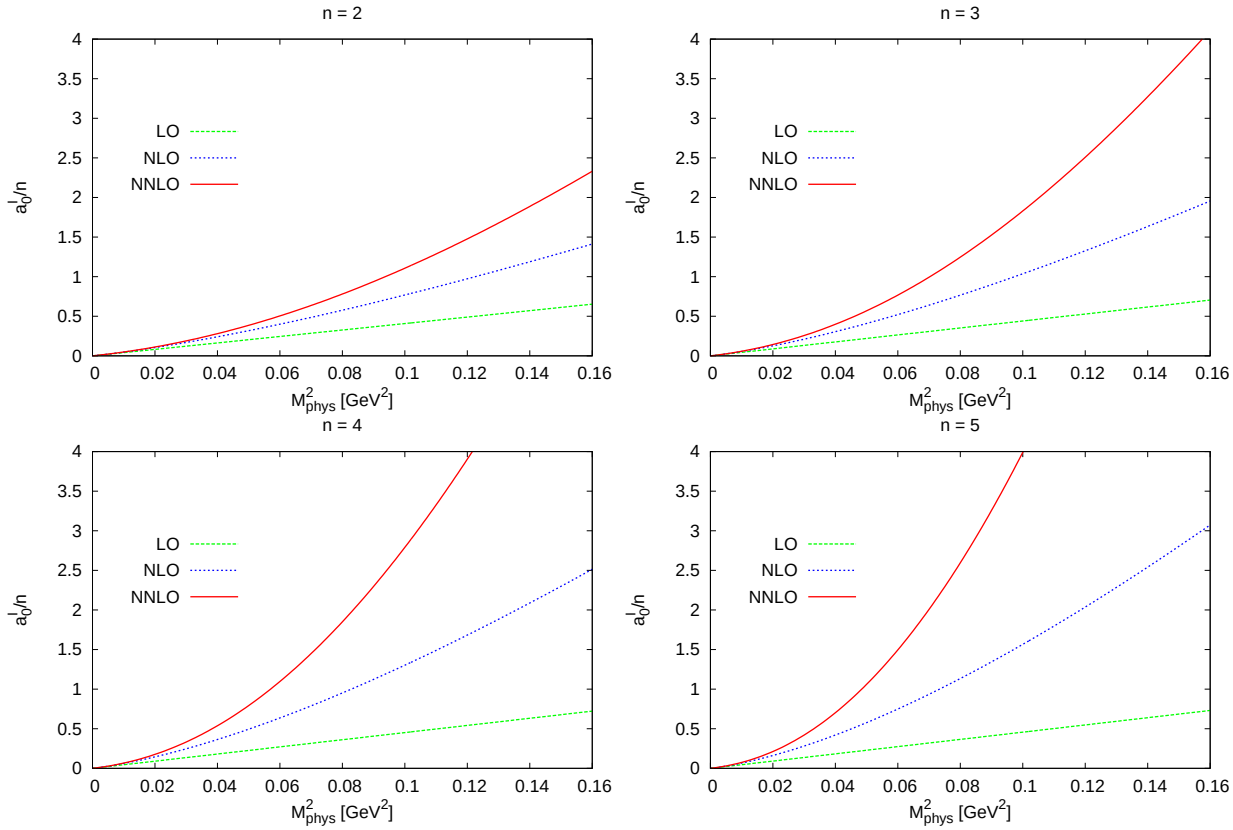

FIGURE 4. The singlet scattering length as a function of the meson mass. The scale is set by the decay constant $F \approx F_\pi$. Plots from [44]. For technicolour applications the mass and decay constant should be scaled up accordingly.

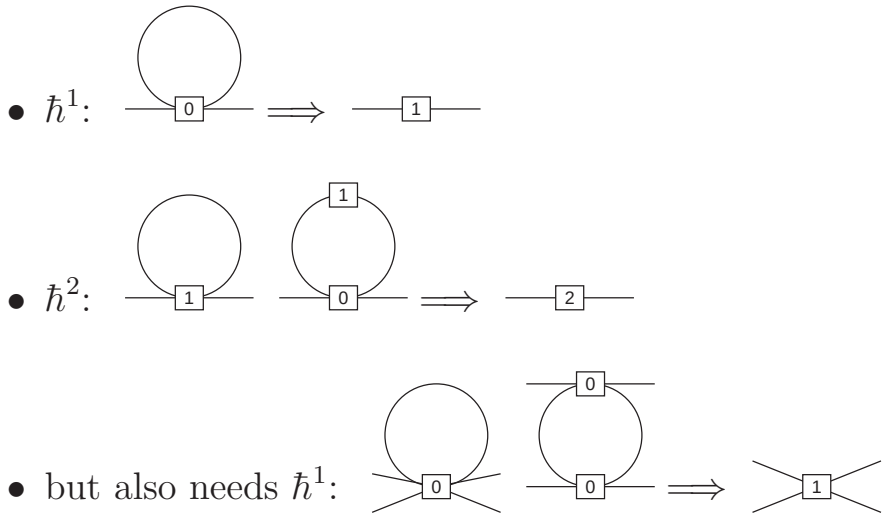

FIGURE 5. The reason for the increase in complexity with the loop-order for leading logarithms in EFT. The index in the vertices shows the loop-order of the vertex needed. Top line: at one-loop we need the one-loop diagram for the and it gives us the mass one-loop counter-term and logarithm. Middle line: at two-loop order we need the two one-loop diagrams to get the two-loop mass counter-term and leading logarithm. It needs the one-loop scattering counter-term as well. Bottom line: the extra one-loop diagrams needed to get one-loop scattering counter-term.

TABLE 3. The coefficients a_i of the leading logarithms for the mass in the massive $O(N)$ model to five loops. Table adapted from [49].

i	a_i, $N=3$	a_i for general N
1	$-\frac{1}{2}$	$1-\frac{N}{2}$
2	$\frac{17}{8}$	$\frac{7}{4}-\frac{7N}{4}+\frac{5\,N^2}{8}$
3	$-\frac{103}{24}$	$\frac{37}{12}-\frac{113N}{24}+\frac{15\,N^2}{4}-N^3$
4	$\frac{24367}{1152}$	$\frac{839}{144}-\frac{1601\,N}{144}+\frac{695\,N^2}{48}-\frac{135\,N^3}{16}+\frac{231\,N^4}{128}$
5	$-\frac{8821}{144}$	$\frac{33661}{2400}-\frac{1151407\,N}{43200}+\frac{197587\,N^2}{4320}-\frac{12709\,N^3}{300}+\frac{6271\,N^4}{320}-\frac{7\,N^5}{2}$

Actually, in the massless case matters simplify somewhat, no vertices with more external legs are needed than already appear at one-loop. The reason is that massless tadpoles vanish. This was used first in [50] for the scalar two-point function LL to five loops. In [51, 52, 53, 54] a clever Legendre polynomial parametrization of the meson-meson scattering vertices allowed to obtain the divergences at all orders via a recursion relation that in some limits can even be solved analytically. Large N in the sigma model agreed with the older work, see e.g. [55]. Treated were meson-meson scattering, scalar and vector form-factors. It was typically found that large N is not a good approximation.

We realized in [49] that a construction of a minimal Lagrangian at each order is not necessary. When calculating the divergences using a method that preserves the underlying symmetry the produced divergence structure will automatically have the correct symmetry and reducing it to its most minimal form or even rewriting it in a fully symmetric form is not needed. The consequence is that things can be computerized and simply let run using FORM [56]. We first pushed the massive nonlinear $O(N)$ model to rather large orders for the masses, form-factors and scattering in [49, 57] and solved the large N-limit to all orders also for the massive case using gap equation techniques. A very strong check of the result is to use different parametrizations of the lowest-order Lagrangian. This should give the same results in the end but intermediate expressions are very different.

An example result is the mass to fifth order via

$$M^2_{\rm phys} = M^2(1+a_1L_M+a_2L_M^2+a_3L_M^3+...) \tag{13}$$

The coefficients a_i are shown in Tab. 3 to five loops. The effects of the anomaly were added in [58]. An example is the pion coupling to two off-shell photons:

$$\begin{aligned} A(\pi^0\to\gamma(k_1)\gamma(k_2)) &= \varepsilon_{\mu\nu\alpha\beta}\,\varepsilon_1^{*\mu}(k_1)\varepsilon_2^{*\nu}(k_2)\,k_1^\alpha k_2^\beta\,F_{\pi\gamma\gamma}(k_1^2,k_2^2)\,, \\ F_{\pi\gamma\gamma}(k_1^2,k_2^2) &= \frac{e^2}{4\pi^2F_\pi}\hat{F}F_\gamma(k_1^2)F_\gamma(k_2^2)F_{\gamma\gamma}(k_1^2,k_2^2)\,. \end{aligned} \tag{14}$$

$\hat{F}$: is for on-shell photons; $F_\gamma(k^2)$ is the form factor for one-off shell photon ; $F_{\gamma\gamma}$ is the nonfactorizable part when both photons are off-shell. This was done to six loops. The on-shell decays leading logarithm part converges extremely well:

$$F = 1+0-0.000372+0.000088+0.000036+0.000009+0.0000002+\ldots \tag{15}$$

The nonfactorizable starts only at three loops and in the massless case only at four loops. The leading logarithms give for this a very small contribution.

The extension to the $SU(N)\times SU(N)$ case was done in [59]. In particular we pushed $\gamma\gamma\to\pi\pi$ there to high order and found only small corrections. A summary of existing massive leading logarithms from our work is:

- $O(N)/O(N-1)$ model [49, 57]
  - massive case: $\pi\pi$, F_V and F_S to 4-loop order
  - large N for these cases also for massive $O(N)$.
  - done using bubble resummations or recursion equation which can be solved analytically
- [58]
  - $O(N)/O(N-1)$ model: Mass, F_π, F_V to six loops

- $O(4)/O(3)$ Anomaly: $\gamma^*3\pi$ (five) and $\pi^0\gamma^*\gamma^*$ (six loops)

• $SU(N)\times SU(N)/SU(N)$ [59]
- Mass, Decay constants, Form-factors
- Meson-Meson, $\gamma\gamma\to\pi\pi$

Typically, the expected radius of convergence was found. Large N was not a good numerical guide either to the actual coefficients unless one went to rather large values of N.

Unfortunately, in no case could we identify a conjecture for all order behaviour of leading logarithms. I strongly recommend all of you to have a look at the many tables in the mentioned papers to see if you have more luck there.

A final comment is that the method has recently been extended to the nucleon sector [60]. This is discussed in more detail in the parallel session talk by A.A. Vladimirov.

7. CONCLUSIONS

In this talk I gave a very short introduction to Chiral Perturbation Theory in the mesonic sector and discussed a number of recent advances. These include the latest determination of the LECs of [8]. Finite volume effects with twisted boundary conditions and preliminary results on the finite volume two-loop results in three flavour ChPT were the next topic. The third subject was the use of mesonic ChPT and its extension to different symmetry breaking patterns with an eye towards applications relevant to technicolour. The last topic was the calculation of leading logarithms in a number of effective field theories to high orders.

ACKNOWLEDGMENTS

I like to thank the organizers for a very pleasant conference and the invitation to present this talk. I also thank my collaborators whose work I have presented here and especially J. Vermaseren, this work would not have been possible without FORM [56]. This work is supported in part by the European Community-Research Infrastructure Integrating Activity "Study of Strongly Interacting Matter" (HadronPhysics3, Grant Agreement No. 283286) and the Swedish Research Council grants 621-2011-5080 and 621-2013-4287.

REFERENCES

1. S. Weinberg, Physica A **96**, 327 (1979).
2. J. Gasser and H. Leutwyler, Annals Phys. **158**, 142 (1984).
3. J. Gasser and H. Leutwyler, Nucl. Phys. B **250**, 465 (1985).
4. H. Leutwyler, Annals Phys. **235**, 165 (1994) [hep-ph/9311274].
5. `http://www.thep.lu.se/~bijnens/chpt/`.
6. J. Bijnens, G. Colangelo and G. Ecker, JHEP **9902**, 020 (1999) [hep-ph/9902437].
7. J. Bijnens, Prog. Part. Nucl. Phys. **58**, 521 (2007) [hep-ph/0604043].
8. J. Bijnens and G. Ecker, arXiv:1405.6488 [hep-ph], to be published in Ann. Rev. Nucl. Part. Sc.
9. G. Colangelo, J. Gasser and H. Leutwyler, Phys. Lett. B **488**, 261 (2000) [hep-ph/0007112].
10. J. Nebreda, J. R. Pelaez and G. Rios, Phys. Rev. D **88**, 054001 (2013) [arXiv:1205.4129 [hep-ph]].
11. S. Aoki *et al.*, Eur. Phys. J. C **74**, no. 9, 2890 (2014) [arXiv:1310.8555 [hep-lat]].
12. J. Bijnens, G. Colangelo and P. Talavera, JHEP **9805**, 014 (1998) [hep-ph/9805389].
13. J. Bijnens and P. Talavera, Nucl. Phys. B **489**, 387 (1997) [hep-ph/9610269].
14. M. Gonzalez-Alonso, A. Pich and J. Prades, Phys. Rev. D **78**, 116012 (2008) [arXiv:0810.0760 [hep-ph]].
15. G. Amorós, J. Bijnens and P. Talavera, Nucl. Phys. B **585**, 293 (2000) [Erratum-ibid. B **598**, 665 (2001)] [hep-ph/0003258].
16. G. Amorós, J. Bijnens and P. Talavera, Nucl. Phys. B **602**, 87 (2001) [hep-ph/0101127].
17. J. Bijnens and I. Jemos, Nucl. Phys. B **854**, 631 (2012) [arXiv:1103.5945 [hep-ph]].
18. J. Bijnens and F. Borg, Eur. Phys. J. C **40**, 383 (2005) [hep-ph/0501163].
19. V. Cirigliano, G. Ecker, H. Neufeld, A. Pich and J. Portoles, Rev. Mod. Phys. **84**, 399 (2012) [arXiv:1107.6001 [hep-ph]].
20. J. Bijnens and I. Jemos, Eur. Phys. J. C **64**, 273 (2009) [arXiv:0906.3118 [hep-ph]].
21. M. Luscher, Commun. Math. Phys. **104**, 177 (1986).
22. J. Gasser and H. Leutwyler, Phys. Lett. B **184**, 83 (1987).
23. J. Gasser and H. Leutwyler, Nucl. Phys. B **307**, 763 (1988).
24. M. Golterman, "Applications of chiral perturbation theory to lattice QCD," arXiv:0912.4042 [hep-lat].

25. D. Becirevic and G. Villadoro, Phys. Rev. D **69**, 054010 (2004) [hep-lat/0311028].
26. S. Descotes-Genon, Eur. Phys. J. C **40**, 81 (2005) [hep-ph/0410233].
27. G. Colangelo, S. Durr and C. Haefeli, Nucl. Phys. B **721**, 136 (2005) [hep-lat/0503014].
28. G. Colangelo and C. Haefeli, Nucl. Phys. B **744**, 14 (2006) [hep-lat/0602017].
29. J. Bijnens and K. Ghorbani, Phys. Lett. B **636**, 51 (2006) [hep-lat/0602019].
30. G. Colangelo, U. Wenger and J. M. S. Wu, Phys. Rev. D **82**, 034502 (2010) [arXiv:1003.0847 [hep-lat]].
31. C. T. Sachrajda and G. Villadoro, Phys. Lett. B **609**, 73 (2005) [hep-lat/0411033].
32. P. F. Bedaque, Phys. Lett. B **593**, 82 (2004) [nucl-th/0402051].
33. J. Bijnens and J. Relefors, JHEP **1405**, 015 (2014) [arXiv:1402.1385 [hep-lat], arXiv:1402.1385].
34. F.-J. Jiang and B. C. Tiburzi, Phys. Lett. B **645**, 314 (2007) [hep-lat/0610103].
35. J. Bijnens and T. Rössler, to be published.
36. J. Bijnens, E. Boström and T. A. Lähde, JHEP **1401**, 019 (2014) [arXiv:1311.3531 [hep-lat]].
37. M. E. Peskin, Nucl. Phys. B **175**, 197 (1980).
38. J. Preskill, Nucl. Phys. B **177**, 21 (1981).
39. S. Dimopoulos, Nucl. Phys. B **168**, 69 (1980).
40. J. B. Kogut, M. A. Stephanov, D. Toublan, J. J. M. Verbaarschot and A. Zhitnitsky, Nucl. Phys. B **582**, 477 (2000) [arXiv:hep-ph/0001171].
41. J. Bijnens, G. Colangelo, G. Ecker, J. Gasser and M. E. Sainio, Nucl. Phys. B **508**, 263 (1997) [Erratum-ibid. B **517**, 639 (1998)] [hep-ph/9707291].
42. J. Bijnens, G. Colangelo, G. Ecker, J. Gasser and M. E. Sainio, Phys. Lett. B **374**, 210 (1996) [hep-ph/9511397].
43. J. Bijnens and J. Lu, JHEP **0911**, 116 (2009) [arXiv:0910.5424 [hep-ph]].
44. J. Bijnens and J. Lu, JHEP **1103**, 028 (2011) [arXiv:1102.0172 [hep-ph]].
45. J. Bijnens and J. Lu, JHEP **1201**, 081 (2012) [arXiv:1111.1886 [hep-ph]].
46. J. Bijnens, G. Colangelo and G. Ecker, Annals Phys. **280**, 100 (2000) [hep-ph/9907333].
47. J. Bijnens, G. Colangelo and G. Ecker, Phys. Lett. B **441**, 437 (1998) [hep-ph/9808421].
48. M. Buchler and G. Colangelo, Eur. Phys. J. C **32**, 427 (2003) [hep-ph/0309049].
49. J. Bijnens and L. Carloni, Nucl. Phys. B **827**, 237 (2010) [arXiv:0909.5086 [hep-ph]].
50. M. Bissegger and A. Fuhrer, Phys. Lett. B **646**, 72 (2007) [hep-ph/0612096].
51. N. Kivel, M. V. Polyakov and A. Vladimirov, Phys. Rev. Lett. **101**, 262001 (2008) [arXiv:0809.3236 [hep-ph]].
52. N. A. Kivel, M. V. Polyakov and A. A. Vladimirov, JETP Lett. **89**, 529 (2009) [arXiv:0904.3008 [hep-ph]].
53. J. Koschinski, M. V. Polyakov and A. A. Vladimirov, Phys. Rev. D **82**, 014014 (2010) [arXiv:1004.2197 [hep-ph]].
54. M. V. Polyakov and A. A. Vladimirov, Theor. Math. Phys. **169**, 1499 (2011) [arXiv:1012.4205 [hep-th]].
55. S. R. Coleman, R. Jackiw and H. D. Politzer, Phys. Rev. D **10**, 2491 (1974).
56. J. A. M. Vermaseren, "New features of FORM," math-ph/0010025.
57. J. Bijnens and L. Carloni, Nucl. Phys. B **843**, 55 (2011) [arXiv:1008.3499 [hep-ph]].
58. J. Bijnens, K. Kampf and S. Lanz, Nucl. Phys. B **860**, 245 (2012) [arXiv:1201.2608 [hep-ph]].
59. J. Bijnens, K. Kampf and S. Lanz, Nucl. Phys. B **873**, 137 (2013) [arXiv:1303.3125 [hep-ph]].
60. J. Bijnens and A. A. Vladimirov, arXiv:1409.6127 [hep-ph].